

Spectral-Energy Efficiency Tradeoff in Multicell Cellular Networks with Adaptive Relay Cooperation

Ivan Ku¹, Cheng-Xiang Wang¹, and John Thompson²

¹Joint Research Institute for Signal and Image Processing, Heriot-Watt University, Edinburgh, EH14 4AS, UK.

²Joint Research Institute for Signal and Image Processing, University of Edinburgh, Edinburgh, EH9 3JL, UK.

Email: {ccik1, cheng-xiang.wang}@hw.ac.uk, {john.thompson}@ed.ac.uk

Abstract—By observing that the relay stations (RSs) will receive a signal replica of the users' transmissions during the broadcast phase, we propose an adaptive relay cooperation scheme. The RSs will utilize the readily available signal replica and the additional diversity naturally inherent in them to either perform cooperative multipoint (COMP) relaying or remain silent with only the direct transmission being considered. We investigate this scheme in a 7 cell network to demonstrate system level capacity and energy efficiency improvements. Results show that the proposed scheme outperforms the conventional adaptive relay scheme and is able to benefit from the more aggressive full bandwidth frequency reuse plan at low relay transmit power.

Index Terms – Green communication, adaptive relay cooperation, MIMO, spectral-energy efficiency tradeoff.

I. INTRODUCTION

First pioneered by [1], wireless relaying is now envisioned in the Long Term Evolution-Advanced (LTE-A) standards and beyond. Regardless of the forwarding mechanisms, a portion of the radio resources will be allocated to the RSs during each transmission frame. Conventionally, RSs operate independently and radio resources that are orthogonal in time or frequency are allocated exclusively to these RSs to minimize interference [2]–[4]. Consequently, system performance may not improve significantly despite registering gains for the individual relay links. To overcome this problem, the RSs must ideally share the same relay slots to better utilize scarce radio resources. However, this comes at a cost of increased interference. In [5], the independent RSs share relay slots and interference was controlled by managing the number of interfering relays.

Recently, much attention is given to cooperative communication as it promises significant throughput improvement. In cooperative relaying, our work focusses on the possibility that the RSs share not only relay slots but also information to perform joint transmission to the user equipments (UEs), thus being a form of COMP relaying. In [6], the spectral efficiency of a flexible downlink resource management scheme for cooperative RSs was evaluated for a single cell whereby a few RSs were utilized to meet a minimum signal quality target at the UE. In [7], inter-cell relay cooperation in forming the uplink precoders to maximize the signal-to-interference-plus-noise ratio (SINR) was investigated and its transmission rate was evaluated for a linear 3 cell topology. The authors in [8] demonstrated energy efficiency improvement through a com-

bination of relay selection and cooperative relay beamforming in a linear topology. Other forms of cooperative transmissions were explored in [9]–[12].

While green radio advocates the importance of energy efficiency [13], an evaluation based on joint spectral-energy efficiency performance is essential as networks of today are constrained by both power and bandwidth. In [14], a multiple antenna decode-and-forward relay system was considered whereby one BS desires to transmit to one UE with the help of the RSs. A subgroup of RSs, selected based on their success to individually decode the BS signal, then cooperatively relay the signal to the UE. In [15] a network consisting of multiple BSs, RSs and UEs, each having multiple antennas, was considered. Each BS desires to transmit to its own UE with the help of a very large group of RSs. During the relay phase, all RSs in the group will cooperatively beamform their signals towards the UEs. In these works, only radio frequency (RF) transmit power is considered when evaluating the spectral-energy efficiency performance. Circuit power, especially in multiple-input multiple-output (MIMO) systems, consumes a sizeable amount of the input power and has begun to be adopted in energy efficiency evaluation [13]. Furthermore, these relay cooperation schemes were not evaluated in a multicell cellular network topology.

In this paper, we propose an adaptive relay cooperation (ARC) scheme for a multicell cellular network. Utilizing the signal replica of the UEs obtained through cooperative decoding during the broadcast phase and their naturally inherent spatial diversity, the RSs will either cooperatively transmit or remain silent so that only the BS direct transmission is considered. We will outline the relay cooperative mechanism and evaluate both its system level information-theoretic capacity and energy efficiency by considering the operational power (RF and circuit powers) and frequency reuse plans.

The rest of the paper is organized as follows. Section II describes the system model and the proposed relay cooperation scheme. In Section III, the interference for various frequency reuse patterns is analysed. The power consumption model is described in Section IV while simulation results are discussed in Section V. Finally, the paper concludes in Section VI.

II. SYSTEM MODEL

Let us consider a multicell cellular network with 7 cells of set $\mathcal{V} \subseteq \{1, \dots, 7\}$. We have 3 sectors of set $\mathcal{U} \subseteq \{1, 2, 3\}$ in

a cell. Each sector has M RSs of set $\mathcal{W} \subseteq \{1, \dots, M\}$ and K UEs of set $\mathcal{K} \subseteq \{1, \dots, K\}$. One BS with n_T antennas per sector is located in the middle of each cell. The number of antennas at the RS and UE are n_R and n_D , respectively. For practical reasons, a half-duplex transmission mode is assumed for the RSs. The time duration of each transmission frame is assumed to be shorter than the coherence time of the channel.

A. Adaptive Relay Cooperation

Let us define $\mathbf{H}_{b,r(m)} \in \mathbb{C}^{n_R \times n_T}$, $\mathbf{H}_{b,u(k)} \in \mathbb{C}^{n_D \times n_T}$ and $\mathbf{H}_{r(m),u(k)} \in \mathbb{C}^{n_D \times n_R}$ as the channel matrices from the BS to the m th RS, the BS to the k th UE and the m th RS to the k th UE of a particular sector in a cell, respectively, where $m \in \mathcal{W}$ and $k \in \mathcal{K}$. It is assumed that the RSs are able to share the channel state information (CSI) and data through the cooperative link that is formed between them. This cooperative link can be a high capacity wireless conference channel that utilizes a different bandwidth than the cellular network. The transmission occurs in a time division multiple access (TDMA) manner as illustrated in Fig. 1(a). During each broadcast phase φ_k , the BS transmits the k th UE signal orthogonally in time while the RSs listen and cooperatively decode the broadcast signal. Therefore, the sum capacity of the broadcast phases is

$$C_{BC} = \sum_{k=1}^K \tau_k \log_2 \left| \mathbf{I}_{Mn_R} + \frac{P_T \mathbf{G}_{\varphi_k} \mathbf{G}_{\varphi_k}^H}{n_T (\mathbf{R}_{BC}^{\varphi_k} + N_0 B \mathbf{I}_{Mn_R})} \right| \quad (1)$$

where τ_k , P_T , B and N_0 are the fraction of time used during the φ_k th broadcast phase, effective BS transmit power, system bandwidth and noise power spectral density, respectively. Note that all capacities here have unit of bits/s/Hz. The effective channel matrix of $\mathbf{G}_{\varphi_k} = [\mathbf{H}_{b,r(1),\varphi_k}^T \cdots \mathbf{H}_{b,r(M),\varphi_k}^T]^T$ is the cascaded channel matrix between the BS and RSs during the φ_k th broadcast phase. The transpose, Hermitian transpose and determinant of a matrix are represented by $(\cdot)^T$, $(\cdot)^H$ and $|\cdot|$, respectively, while \mathbf{I}_m denotes the identity matrix of size $m \times m$. The interference covariance matrix $\mathbf{R}_{BC}^{\varphi_k}$ and also those hereafter will be evaluated in the next section. We also consider the direct link from the BS to the UEs in which case the RSs will be silent if this direct link capacity is higher than that achieved by relaying. The direct link sum capacity is given as

$$C_{BCD} = \sum_{k=1}^K \tau_k \log_2 \left| \mathbf{I}_{n_D} + \frac{P_T \mathbf{H}_{b,u(k),\varphi_k} \mathbf{H}_{b,u(k),\varphi_k}^H}{n_T (\mathbf{R}_D^{\varphi_k} + N_0 B \mathbf{I}_{n_D})} \right|. \quad (2)$$

During the relay phase represented by Phase φ_R in Fig. 1(a), the RSs occupy the same relay slot to cooperatively relay to the UEs. Let $\mathbf{F}_k = [\mathbf{H}_{r(1),u(k),\varphi_R} \cdots \mathbf{H}_{r(M),u(k),\varphi_R}]$ be the effective channel matrix between the RSs and the k th UE. The RSs jointly calculate the precoder matrix \mathbf{W}_k in order to maximize the sum capacity of the relay phase given as

$$C_R = \max \sum_{k=1}^K f \tau_R \log_2 \left| \mathbf{I}_{n_D} + \frac{\mathbf{S}_k \mathbf{S}_k^H}{(\mathbf{R}_R^k + N_0 B f \mathbf{I}_{n_D})} \right| \quad (3)$$

where f is the frequency reuse factor depending upon the relay frequency reuse (RFR) pattern, $\mathbf{S}_k = \mathbf{F}_k \mathbf{W}_k$ and τ_R is the fraction of time used during the relay phase. Note that $\sum_{k=1}^K \tau_k + \tau_R = 1$. Assuming the interval is equal for all K UEs, we have $\tau_k = \frac{1-\tau_R}{K}$. Without intra-cell interference, the condition $\mathbf{F}_l \mathbf{W}_k = \mathbf{0} : l \in \mathcal{K}, l \neq k$ and $K \leq \left\lceil \frac{n_R M}{n_D} \right\rceil$ must be met, with $\lceil \cdot \rceil$ being the ceiling operator. Let's define $\tilde{\mathbf{F}}_k = [\mathbf{F}_1^T \cdots \mathbf{F}_{k-1}^T \mathbf{F}_{k+1}^T \cdots \mathbf{F}_K^T]^T$. The solution for \mathbf{W}_k that will maximize the sum capacity and simultaneously suppress intra-cell interference is obtained through the combination of the singular vector decomposition (SVD) and water-filling approaches. For each k , we obtain the right singular vector null spaces, $\tilde{\mathbf{V}}_k^{\text{null}}$ by SVD of $\tilde{\mathbf{F}}_k$. Next, the SVD $(\mathbf{F}_k \tilde{\mathbf{V}}_k^{\text{null}})$ is evaluated and the singular value diagonal matrix, $\tilde{\Gamma}_k \in \mathbb{R}^{r \times r}$ and its corresponding first r right singular vectors $\tilde{\mathbf{V}}_k^{\text{base}}$ are extracted, whereby $r = \text{rank}(\mathbf{F}_k \tilde{\mathbf{V}}_k^{\text{null}})$. Water filling is then applied to the diagonal elements of $\tilde{\Gamma}_k$ to produce the power allocation matrix, Π_k , that satisfies the power constraint $\sum_{k=1}^K \text{trace}(\mathbf{W}_k \mathbf{W}_k^H) = M P_R$, where P_R is the effective RS transmit power. Finally, the k th precoder matrix is obtained as $\mathbf{W}_k = \tilde{\mathbf{V}}_k^{\text{null}} \tilde{\mathbf{V}}_k^{\text{base}} \Pi_k^{1/2}$. The capacity of the relay cooperation is then calculated as

$$C_{RCoop} = \max \{ \min \{ C_{BC}, C_R \}, C_{BCD} \}. \quad (4)$$

For the UEs that are located near the BS or have a high quality BS link, the use of relays becomes redundant as relay systems will incur multiplexing loss due to the two-hop requirement. In this case, we will switch to purely direct transmission mode whose sum capacity is given as

$$C_D = \frac{1}{K} \sum_{k=1}^K \log_2 \left| \mathbf{I}_{n_D} + \frac{P_T \mathbf{H}_{b,u(k),\varphi_k} \mathbf{H}_{b,u(k),\varphi_k}^H}{n_T (\mathbf{R}_D^{\varphi_k} + N_0 B \mathbf{I}_{n_D})} \right|. \quad (5)$$

Thus, the overall capacity for the adaptive relay cooperation (ARC) scheme is

$$C_{ARC} = \max \{ C_{RCoop}, C_D \}. \quad (6)$$

III. INTERFERENCE ANALYSIS

We now analyze the interference when using different RFR patterns in order to evaluate performance of the scheme at the system level. We start by defining the channel matrix in more detail. Let $\mathbf{H}_{X,Y} \in \mathbb{C}^{A \times B}$ be the channel matrix between nodes X and Y. The elements of $\mathbf{H}_{X,Y}$ are $h_{a,b}$ ($1 \leq a \leq A, 1 \leq b \leq B$) and can be expressed by

$$h_{a,b} = G_X \cdot G_Y \cdot (L_{X,Y})^{-1} \cdot 10^{u_{X,Y}/10} \cdot \mu_{X,Y} \quad (7)$$

where G_X and G_Y are the gains of the transmit and receive antennas, respectively. The path loss between X and Y is defined as $L_{X,Y}$. The next term is the log-normal shadowing with $u_{X,Y}$ following the Gaussian distribution with zero mean and standard deviation, σ dB. Lastly, $\mu_{X,Y}$ represents the complex Rayleigh fast fading coefficient with unit variance.

More details of their values are tabulated in Table I. Let us further define $b(i, j)$, $r(i, j, m)$ and $u(i, j, k)$ as the BS from the i th sector of the j th cell, the m th RS from the i th sector of the j th cell and the k th UE from the i th sector of the j th cell, respectively, with $i \in \mathcal{U}$ and $j \in \mathcal{V}$.

It is sufficient to focus on one sector of the base (centre) cell as the performance of other sectors is identical on average. We choose $(i, j) = (1, 1)$ as the base sector (Fig. 1). During the broadcast phases, the BS transmits at a full frequency reuse factor to be spectrally efficient. Interference is commonly minimized through sectorization and deploying high gain directional antennas at the BS. For this transmission phase, the set of interference sources to both the RSs and UEs are from the BSs transmitting at all the sectors across the cells besides the base sector, that is, $\mathcal{X} \subseteq \mathcal{U} \times \mathcal{V} : (i, j) \neq (1, 1)$. Assuming the interference is independent, the interference covariance matrix of the broadcast phase φ_k for the cooperative RSs, $\mathbf{R}_{\text{BC}}^{\varphi_k}$ in (1), is a block diagonal matrix given as

$$\mathbf{R}_{\text{BC}}^{\varphi_k} = \text{diag}[\mathbf{U}_1^{\varphi_k} \mathbf{U}_2^{\varphi_k} \cdots \mathbf{U}_M^{\varphi_k}] \quad (8)$$

where

$$\mathbf{U}_m^{\varphi_k} = \sum_{p \in \mathcal{X}} \frac{P_T}{n_T} \mathbf{H}_{b(p), r(1,1,m), \varphi_k} \mathbf{H}_{b(p), r(1,1,m), \varphi_k}^H \quad (9)$$

while the interference covariance matrix at broadcast phase φ_k for the k th UE, $\mathbf{R}_{\text{D}}^{\varphi_k}$ in (2) and (5) is written as

$$\mathbf{R}_{\text{D}}^{\varphi_k} = \sum_{p \in \mathcal{X}} \frac{P_T}{n_T} \mathbf{H}_{b(p), u(1,1,k), \varphi_k} \mathbf{H}_{b(p), u(1,1,k), \varphi_k}^H \quad (10)$$

During the relay phase φ_R , the set of interference sources are from other RSs not belonging to the base sector which are relaying at the frequency band at which the k th UE in the base sector is currently receiving, that is, $\mathcal{P}_k \subseteq \mathcal{X} \times \mathcal{W} : r(i, j, m)_{\text{freq}} = u(1, 1, k)_{\text{freq}}$. Thus, the interference covariance matrix at relay phase φ_R for the k th UE, \mathbf{R}_{R}^k in (3), can be written as

$$\mathbf{R}_{\text{R}}^k = \sum_{q_k \in \mathcal{P}_k} \frac{P_R}{n_R} \mathbf{H}_{r(q_k), u(1,1,k), \varphi_R} \mathbf{H}_{r(q_k), u(1,1,k), \varphi_R}^H \quad (11)$$

A. Relay Frequency Reuse Pattern

As the RSs' antennas are usually omni-directional, careful relay frequency reuse planning is essential to mitigate interference in the relay phase. Three types of RFR patterns are investigated. We introduce the $f = 1/3$ RFR pattern of Fig. 1(b) (Type I) to work with the proposed ARC scheme. The $f = 1/3$ RFR pattern of Fig. 1(c) (Type II) is commonly utilized by conventional relaying and will be used for comparison purposes. We are also interested in the performance of $f = 1$ RFR pattern of Fig. 1(d) (Type III) whereby the RSs utilize the full bandwidth for relaying.

Firstly, we consider the Type I RFR pattern used in the ARC scheme. With this RFR pattern, inter-cell interference coming from the immediately adjacent sectors around the the base cell can be avoided. The intra-cell interference in each sector due to co-location of the same frequency band is

further eliminated through the proposed ARC scheme which also simultaneously provides additional diversity gain through cooperative relaying. The only interference sources are those coming from the surrounding cells with distances of at least one sector away from the base sector. Given the finite exponent decay of path loss, the outer inter-cell interference sources are usually weak. In contrast, the Type II RFR pattern is adopted by conventional relaying to minimize (but not completely eradicate) intra-cell interference during the relay phase. However, it is not able to avoid inter-cell interference from the immediately adjacent cell sites when a system level perspective is considered as illustrated in Fig. 1(c). Thus, the accumulated interference power in (11) is smaller for the Type I RFR pattern as compared to the Type II RFR pattern. As for the Type III RFR pattern, all the RSs are using the same frequency and time slot for transmission. Because of this, it is spectrally most efficient but incurs the highest accumulated interference power. Therefore, we have

$$\|\mathbf{R}_{\text{R,Type I}}^k\|_{\text{F}} < \|\mathbf{R}_{\text{R,Type II}}^k\|_{\text{F}} < \|\mathbf{R}_{\text{R,Type III}}^k\|_{\text{F}} \quad (12)$$

where $\|\cdot\|_{\text{F}}$ is the Frobenius norm of a matrix. To avoid an excessive level of interference, conventional relay schemes do not usually use the Type III RFR pattern. Nevertheless, the benefit of full bandwidth utilization in Type III RFR pattern can be exploited in the proposed ARC scheme as it is able to remove interference from within its own sector. For completeness, we will also evaluate this RFR pattern with the conventional relaying scheme.

IV. POWER CONSUMPTION MODEL

Unlike prior work in [8] [14] [15], we include both the RF transmit power and the circuit power consumption.

A. Operational Power Consumption

Let P_{BS} , P_{RS} and N_{Sector} be the RF transmit power allocated to the BS for the entire cell, the RF relay power allocated to each RS and the number of sectors per cell, respectively. Also, let α_B and α_R be the effective efficiencies at the BS and RS, respectively, taking into consideration the aggregate effect of the duplexer/feeder losses and the efficiencies of the antenna/amplifier modules. We assume P_{BS} is equally allocated at each sector. Therefore, the effective BS transmit power at each sector is

$$P_T = \frac{P_{\text{BS}}}{N_{\text{Sector}}} \quad (13)$$

We also assume that each sub-channel of the relay phase is allocated equal power. Consequently, the RSs will use a fraction of the allocated P_{RS} according to its RFR pattern. Thus, the effective RS transmit power is

$$P_R = P_{\text{RS}} f \quad (14)$$

where f is determined by the RFR pattern being used as illustrated in Fig. 1. Since the base sector is of primary focus, the total RF transmit power per sector per user is given as

$$P_{\text{RF,Total}} = \begin{cases} \alpha_B P_T \tau_k + \beta \alpha_R P_R \tau_R M K^{-1} & \text{if relay} \\ \alpha_B P_T K^{-1} & \text{if DT} \end{cases} \quad (15)$$

where DT stands for direct transmission and $\beta = \{0, 1\}$ determines whether the relay scheme is using only the direct link ($\beta = 0$) or the full relaying mechanism ($\beta = 1$).

Similar to [16], it is assumed that the circuit power consumption of the BS and RSs is proportional to their effective transmit power defined in (13) and (14). Let $P_{C,\max}$ be the maximum circuit power at maximum transmit power, P_{\max} . Therefore, the total circuit power per sector per user can be written as

$$P_{C,\text{Total}} = \frac{P_{C,\max}}{K P_{\max}} (P_T + M P_R). \quad (16)$$

Finally the operational power consumption per sector per user, calculated by summing (15) and (16), is given as

$$P_{\text{Op}} = P_{\text{RF,Total}} + P_{C,\text{Total}} = \begin{cases} P_T \left(\alpha_B \tau_k + \frac{P_{C,\max}}{K P_{\max}} \right) + \frac{P_R M}{K} \left(\beta \alpha_R \tau_R + \frac{P_{C,\max}}{P_{\max}} \right) & \text{if relay,} \\ \frac{P_T}{K} \left(\alpha_B + \frac{P_{C,\max}}{P_{\max}} \right) + \frac{P_R M P_{C,\max}}{K P_{\max}} & \text{if DT.} \end{cases} \quad (17)$$

After some algebraic manipulation, the first and second terms of each piecewise equation in (17) are the BS and RSs operational power per sector per user, respectively. It is observed that although the direct transmission mode is selected, the RSs are still turned on. Thus, the RSs' circuit power consumption remains in this case.

B. Energy Consumption Ratio

The energy consumption ratio (ECR) is used to measure the energy efficiency of the system. It is proportional to the ratio of the average operational power to the average capacity of the system. For a given system bandwidth, B , the ECR for the ARC scheme is thus

$$\text{ECR}_{\text{ARC}} = \frac{\mathbb{E}\{P_{\text{Op}}\}}{B \cdot \mathbb{E}\{C_{\text{ARC}}\}} \quad (18)$$

where $\mathbb{E}\{\cdot\}$ is the expectation operator. The ECR metric has a unit of J/bit.

V. SIMULATION RESULTS AND ANALYSIS

In our simulations, each sector has two RSs ($M = 2$) and two randomly dropped UEs ($K = 2$), their positions being uniformly distributed. We compare the ARC scheme against the conventional adaptive relay (AR) scheme. The AR scheme also switches between relaying and direct transmission but its RSs operate independently in exclusive relay slots. Table I lists the rest of the simulation parameters.

In Fig. 2, the 10% outage capacity of the schemes is shown. At $P_{RS} = 2\text{W}$ in Fig. 2(a), the ARC scheme outperforms the AR scheme by 4% and 10% for $f = 1/3$ and $f = 1$, respectively. As f goes from $1/3$ to 1 , the ARC scheme improves by 22% while the AR scheme achieves a 16% higher data rate. Therefore, the ARC scheme is better at suppressing intra-cell and strong inter-cell interferences through its Type

I RFR pattern with relay cooperation. The aggressive full bandwidth Type III RFR pattern is also exploited by the ARC scheme by mitigating intra-cell interference through relay cooperation. The benefit of the ARC scheme over the AR scheme is observed again in Fig. 2(b) at $P_{RS} = 6\text{W}$ albeit a 2% reduction in gains due to stronger interference. Increasing P_{RS} from 2W to 6W while maintaining the RFR patterns achieves only marginal capacity gains. Thus, adopting a full bandwidth RFR pattern achieves higher capacity gains than increasing relay transmit power, especially at low P_{RS} .

The average sector capacity and energy efficiency are shown in Fig. 3. For $f = 1/3$ and $P_{RS} = 2\text{W}$ in Fig. 3(a), the capacity of the AR scheme saturates at 2.51 bits/s/Hz with an ECR of 9.8 $\mu\text{J}/\text{bit}$ while the ARC scheme achieves a similar capacity at 3.6 $\mu\text{J}/\text{bit}$. At $f = 1$, the capacity of the AR scheme saturates at 2.63 bits/s/Hz with an ECR of 10.8 $\mu\text{J}/\text{bit}$ while the ARC scheme requires 2.7 $\mu\text{J}/\text{bit}$ for the same capacity. Furthermore, at 3.6 $\mu\text{J}/\text{bit}$ the capacity of the ARC scheme improves by 11% as it switches from $f = 1/3$ to $f = 1$ while the AR scheme gains only 3%. Thus, while the ARC scheme is more energy efficient than the AR scheme with reuse factor $f = 1/3$, further capacity and energy efficiency gains are achieved for a reuse factor $f = 1$. At $P_{RS} = 6\text{W}$ in Fig. 3(b), we see the same energy saving trend but at higher energy per bit values. Going from $P_{RS} = 2\text{W}$ to $P_{RS} = 6\text{W}$ while maintaining the same RFR pattern, an overall loss in energy efficiency is observed as the interference strength is increased. A higher energy per bit is required at $P_{RS} = 6\text{W}$ to achieve the same capacity as when $P_{RS} = 2\text{W}$, with the $f = 1$ RFR patterns leading to higher energy consumption. Therefore, utilizing the full bandwidth RFR pattern is more energy efficient at low P_{RS} while partial bandwidth RFR pattern ($f = 1/3$) is favoured at high P_{RS} though at lower energy efficiency.

VI. CONCLUSIONS

An ARC scheme with two different frequency reuse plans has been proposed whereby the relays either perform cooperative relaying to the users or remain silent while direct transmission is considered if the direct link capacity is high. The system level capacity and energy efficiency have been jointly evaluated and compared with the conventional AR scheme with independent relaying. Results have shown that relay slot sharing with cooperative transmission in the proposed scheme outperforms individual relay slot allocation with no relay cooperation represented by the conventional relay scheme, with full bandwidth frequency reuse planning and low relay transmit power being favoured.

ACKNOWLEDGEMENTS

This work has formed part of the Green Radio Core 5 Research Programme of Mobile VCE (www.mobilevce.com). This research has been funded by the industrial members of Mobile VCE and the ES-PRC. Support by the Scottish Funding Council for the Joint Research Institute in Signal and Image Processing, as part of the Edinburgh Research Partnership in Engineering and Mathematics (ERPem), and

by the RCUK for the UK-China Science Bridges Project: R&D on (B)4G Wireless Mobile Communications is acknowledged.

REFERENCES

- [1] E. C. van der Meulen, "Three-terminal communication channels," *Adv. Appl. Probab.*, vol. 3, pp. 120–154, 1971.
- [2] J. Hu and N. C. Beaulieu, "Performance analysis of decode-and-forward relaying with selection combining," *IEEE Commun. Letters*, vol. 11, no. 6, pp. 489–491, June 2007.
- [3] W.-J. Huang, Y.-W. P. Hong, and C.-C. J. Kuo, "Lifetime maximization for amplify-and-forward cooperative networks," *IEEE Trans. Wireless Commun.*, vol. 7, no. 5, pp. 1800–1805, May 2008.
- [4] Q. Lin, X. Wang, Y. Wang, and J. Liao, "Performance evaluation of frequency planning in a novel cellular architecture based on sector relay," in *Proc. IEEE VTC-Spring'10*, Taipei, Taiwan, May 2010, pp. 1–5.
- [5] A. Austin and J. Vidal, "Amplify-and-forward cooperation under interference-limited spatial reuse of the relay slot," *IEEE Trans. Wireless Commun.*, vol. 7, no. 5, pp. 1952–1962, May 2008.
- [6] Y. Kim, T. Kim, S. Kim, and Y. Han, "Adaptive cooperation strategy for multiple relays in 4G wireless systems," in *Proc. IEEE WCNC'09*, Budapest, Hungary, Apr. 2009, pp. 1–5.
- [7] H. Ganapathy, J. G. Andrews, and C. Caramanis, "Inter-cell relay cooperation in heterogeneous cellular uplink systems," in *Proc. ACSSC'08*, California, USA, Oct. 2008, pp. 1443–1447.
- [8] R. Madan, N. B. Mehta, A. F. Molisch, and J. Zhang, "Energy-efficient cooperative relaying over fading channels with simple relay selection," *IEEE Trans. Wireless Commun.*, vol. 7, no. 8, pp. 3013–3025, Aug. 2008.
- [9] C.-X. Wang, X. Hong, X. Ge, X. Cheng, G. Zhang, and J. S. Thompson, "Cooperative MIMO channel models: A survey," *IEEE Commun. Mag.*, vol. 48, no. 2, pp. 80–87, Feb. 2010.
- [10] X. Ge, K. Huang, C.-X. Wang, X. Hong, and X. Yang, "Capacity analysis of a multi-cell multi-antenna cooperative cellular network with co-channel interference," *IEEE Trans. Wireless Commun.*, vol. 10, no. 10, pp. 3298–3309, Oct. 2011.
- [11] K. Yang, S. Ou, H. Chen, and J. He, "A multihop peer communication protocol with fairness guarantee for IEEE 802.16 based vehicular networks," *IEEE Trans. Veh. Tech.*, vol. 56, no. 6, pp. 3358–3370, Nov. 2007.
- [12] X. Cheng, C.-X. Wang, H. Wang, X. Gao, X.-H. You, D. Yuan, B. Ai, Q. Huo, L. Song, and B. Jiao, "Cooperative MIMO channel modeling and multi-link spatial correlation properties," *IEEE J. Sel. Areas in Commun.*, vol. 30, no. 2, pp. 388–396, Feb. 2012.
- [13] C. Han, T. Harrold, S. Armour, I. Krikidis, S. Videv, P. M. Grant, H. Haas, J. S. Thompson, I. Ku, C.-X. Wang, T. A. Le, M. R. Nakhai, J. Zhang, and L. Hanzo, "Green radio: Radio techniques to enable energy efficient wireless networks," *IEEE Commun. Mag.*, vol. 49, no. 6, pp. 46–54, Jun. 2011.
- [14] X. Lao, L. Cuthbert, T. Zhang, and L. Xiao, "Energy efficiency and optimal resource allocation in cooperative wireless relay networks," in *Proc. IEEE VTC-Spring'11*, Budapest, Hungary, May 2011, pp. 1–6.
- [15] O. Oyman and A. J. Paulraj, "Power-bandwidth tradeoff in dense multi-antenna relay networks," *IEEE Trans. Wireless Commun.*, vol. 6, no. 6, pp. 2282–2293, Jun. 2007.
- [16] I. Ku, C.-X. Wang, J. Thompson, and P. Grant, "Impact of receiver interference cancellation techniques on the base station power consumption in MIMO systems with inter-cell interference," in *Proc. IEEE PIMRC'11*, Toronto, Canada, Sep. 2011, pp. 1798–1802.

TABLE I
SIMULATION PARAMETERS

Parameters	Values	
Cell radius, r_{cell}	2000 m	
Inter-site distance, d_{ISD}	$\sqrt{3}$ of cell radius	
RS distance, d_{RS}	0.7 of cell radius	
BS transmit power, P_{BS}	Maximum 40 W per cell	
RS transmit power, P_{RS}	2 W and 6 W	
Relay time fraction, τ_{R}	1/3	
Number of antennas	$n_T = n_R = n_D = 2$	
Effective BS efficiency, α_{B}	2.84	
Effective RS efficiency, α_{R}	2.84	
Maximum circuit power, $P_{\text{C, max}}$	577 W at $P_{\text{max}} = 40$ W	
Noise power spectral density, N_0	-174 dBm	
System bandwidth, B	10 MHz	
Path loss model (d in km)	BS–RS	$125.2 + 36.3 \log_{10}(d)$ dB
	BS–UE	$131.1 + 42.8 \log_{10}(d)$ dB
	RS–UE	$145.4 + 37.5 \log_{10}(d)$ dB
Shadowing standard deviation	BS–RS	6 dB
	BS–UE	10 dB
	RS–UE	10 dB
Antenna pattern ($\theta_{\text{3dB}} = 70^\circ$, $A_m = 20$ dB)	BS	$\rho(\theta) = -\min\left(12 \left(\frac{\theta}{\theta_{\text{3dB}}}\right)^2, A_m\right)$ dB
	RS–BS	$\rho(\theta) = -\min\left(12 \left(\frac{\theta}{\theta_{\text{3dB}}}\right)^2, A_m\right)$ dB
	RS–UE	Omni
	UE	Omni
Antenna gain (boresight)	BS	14 dBi (including cable losses)
	RS–BS	7 dBi (including cable losses)
	RS–UE	5 dBi (including cable losses)
	UE	0 dBi

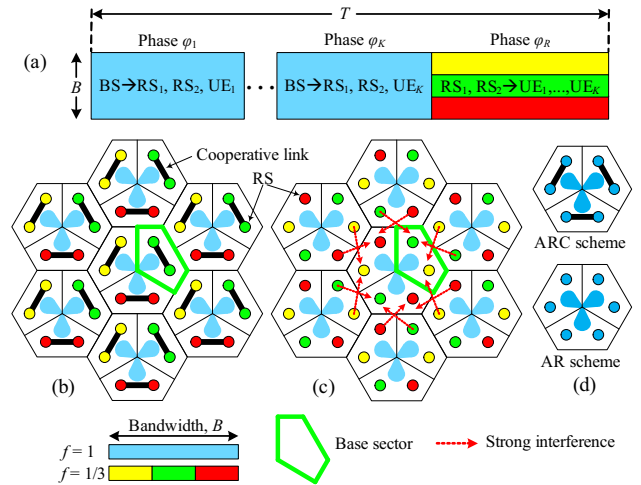


Fig. 1. The ARC scheme's (a) timing protocol at each sector and (b) its Type I relay frequency reuse (RFR) pattern, while (c) shows the Type II RFR pattern of the conventional AR scheme and (d) shows the Type III RFR pattern for both schemes for a single cell ($M = 2$).

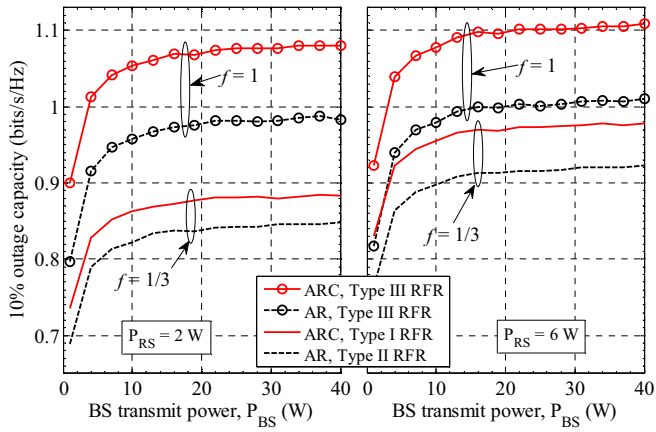


Fig. 2. Outage capacity of the ARC and AR schemes with their corresponding $f = 1/3$ (Type I,II) and $f = 1$ (Type III) RFR patterns at P_{RS} of 2W and 6W for various P_{BS} (figures share common y-axis).

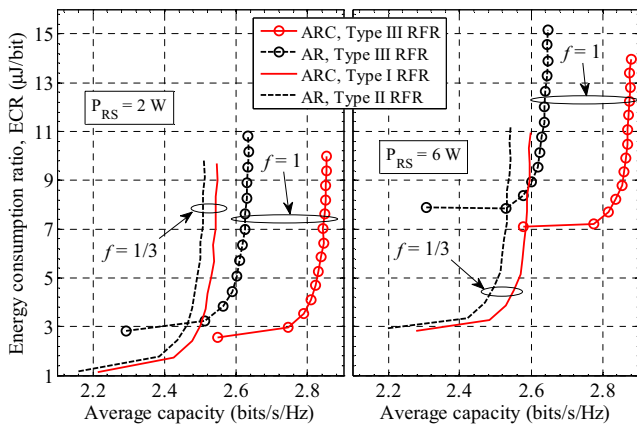


Fig. 3. Energy consumption ratio v.s. average sector capacity of the ARC and AR schemes with their corresponding $f = 1/3$ (Type I,II) and $f = 1$ (Type III) RFR patterns at P_{RS} of 2W and 6W (figures share common y-axis).